Supporting Information

Daskalakis et al. 10.1073/pnas.1401660111

SI Materials and Methods

Behavioral Assessment. The elevated plus-maze (EPM) test was performed as previously described (1, 2). Each test lasted 5 min and was recorded and analyzed with the use of EthoVision automated tracking system (Noldus Information Technology). Behaviors assessed were: time spent in open and closed arms and on the center the platform, number of entries in open or closed arm and total exploration (entries into all arms), and anxiety index [1 – (0.5 [Time in open arms]/5 min) + 0.5 (Open arm entries/Total exploration)] (2). Predator-scent-stress (PSS) exposure increased the time in the open arms in the EPM compared with the PSS-unexposed control (CON) group both in males ($F_{1,\ 49} = 5.3$, $P = 0.030$) and females ($F_{1,\ 52} = 6.8$, $P = 0.015$), with no effect in total exploration of the maze between groups.

The acoustic-startle response (ASR) test was also performed as previously described (1, 2). Behavioral assessment consisted of mean startle amplitude (averaged over 30 trials) and startle habituation to the repeated presentation of the acoustic pulse (100 dB[A] white noise; 40-ms duration). Startle habituation was the percent change between the response to the first block of acoustic pulses (trial 1–5) and the last block (trial 26–30), and was calculated as follows: 100 × [(Average startle amplitude in Block 1) − (Average startle amplitude in Block 6)]/(Average startle amplitude in Block 1). Stress exposure significantly increased the mean startle amplitude and significantly reduced startle habituation in the ASR test in exposed rats compared with CONs in both males ($F_{1,\ 49} = 17.3$, $P < 0.001$ and $F_{1,\ 49} = 7.7$, $P = 0.008$, respectively) and females ($F_{1,\ 52} = 14.6$, $P < 0.001$ and $F_{1,\ 52} = 10.4$, $P = 0.003$, respectively), indicating hyperarousal.

Cut-off behavioral criteria (CBC) were used to classify PSS-exposed rats according to their behavior response on day 7, as previously described (3–6). The same CBC criteria were used for both males and females. Within each sex, PSS-exposed rats were divided in the extreme behavioral response (EBR), minimal behavioral response (MBR), and partial behavioral response (PBR) groups. The graphic representation of the behavioral data (Fig. S1 *C* and *D*) depicts the clustering of individuals with the extreme responses to exposure (reduced time in open arms, high startle amplitude, low startle habituation; the EBRs), apart from the individuals with the minimal response (increased time in open arms, low startle amplitude and high startle habituation; the MBRs). Same type of separation of EBRs from MBRs was observed in both sexes.

Samples Processing. At the time of being killed, 2.5 mL whole peripheral blood from each rat was collected into PAXgene Blood RNA Tubes (Qiagen). Blood samples were incubated at room temperature for 4 h for RNA stabilization (PAXgene RNA stabilization system; Qiagen) and then stored at −80 °C. Total RNA was extracted using the PAXgene Blood RNA Kit (Qiagen) with the addition of on-column DNase digestion. Because there is a predominant presence of globin transcript in whole-blood samples that constitute ∼70% of mRNA, the globin messenger RNA (mRNA) reduction method was used to diminish globin mRNA interference in the blood total RNA (GLOBINclear Mouse/Rat kit; Ambion).

Amygdala and hippocampus were dissected on dry ice using established anatomical landmarks (7). Tissues were immediately submerged in RNA-stabilization solution (RNAlater, Ambion), and stored at −80 °C. RNeasy Mini Kits (Qiagen) were used to isolate total RNA with the addition of on-column DNase digestion.

RNA concentration was determined using a ND-1000 spectrophotometer (NanoDrop Technologies). The purity and quality of the extracted total RNA were evaluated using the RNA 6000 Nano LabChip kit and 2100 Bioanalyzer (Agilent Technologies). High-quality RNA with RNA integrity numbers greater than 8.0 was used in further analyses. Each sample was coded and further analyses were performed blind to groups.

DNA Microarray Analysis. Blood, amygdala, and hippocampus RNA of EBRs, MBRs, and CONs was used for microarray analysis with the Rat Ref-12 Expression BeadChip (Illumina). These chips contain 22,523 probes per array (22,228 genes) selected from the National Center for Biotechnology Information Reference Sequence (RefSeq) database, release 16. Blood and brain RNA samples from males and females were run at the same time (blood: $n = 8$ arrays per group, total of 48 arrays, brain: $n = 5$ arrays per group; total of 90 arrays). Illumina TotalPrep RNA Amplification kit (Ambion) was used to do reverse transcription and in vitro transcription to synthesize cRNA from 200 ng RNA per sample. Briefly, double-stranded cDNA was synthesized using T7-oligo (dT) primers, followed by an in vitro transcription reaction to amplify cRNA while biotin was incorporated into the synthesized cRNA. After purification, the biotinylated cRNA was quantified using a NanoDrop spectrophotometer and the size distributions of cRNA assessed using Bioanalyzer. Then, 1.5 μg biotinylated cRNA was hybridized to Rat Ref-12 Arrays (Illumina). The hybridization, washing, and scanning were performed according to the manufacturer's instructions in the Genomics Core Facility of the Icahn School of Medicine at Mount Sinai. The scanned microarray images were registered and raw data, including the probe signal values and probe detection *P* values were extracted with the use of BeadStudio (Illumina).

Quality control was performed using the dataset preprocessing strategies implemented in the *R* (www.R-project.org) package lumi (8). One array failed (female blood) and one array (male hippocampus) was excluded based on quality control. Because our primary interest was large-scale expression changes, we used the detection *P* values to remove genes that were poorly expressed. We retained probes for which the majority (>50%) of samples from each group displayed a detection *P* value lower than <0.05. Detected probes were called for males and females separately. Fewer genes were detected in blood (approximately 6,000) than in the brain (approximately 10,000) in both sexes.

Quantitative PCR Validation. Quantitative PCR (qPCR) was performed to validate differential gene expression results using the StepOnePlus Real-Time PCR System (Applied Biosystems). We used four biological replicates with two being independent samples from the ones used for the microarrays. cDNA was synthesized by reverse-transcription reaction using the RNA to cDNA Double Primed EcoDry kit (Clontech). Target and reference genes' primers sequence and associated Universal Probe Library (UPL) probes were selected using the ProbeFinder v2.49 web-based software (Roche) and are included in Table S1.

Only one cDNA was amplified in each PCR (monoplex) and samples were analyzed in triplicate. The reactions were quantitated by selecting the amplification cycle when the PCR product of interest is first detected (threshold cycle, Ct). To account for sample-to-sample variability, the expression level of each transcript in each sample was normalized to the geometric mean of the expression levels of two endogenous references (B2M, HPRT1).

Data analysis for qPCR was performed using qBase v2.5 (Biogazelle NV).

Hierarchical Clustering. The U-set sets were overlapped across-tissue and unsupervized hierarchical clustering analysis was performed for the differentially expressed genes (DEG) that belonged in the statistically significant overlaps. For this, standard *z*-scores were calculated from the normalized probe signal values. Clustering of DEG and experimental groups was prepared with CIMminer software (Genomics and Bioinformatics Group, Laboratory of Molecular Pharmacology, Center for Cancer Research, National Cancer Institute) using the default setting (distance method: Euclidean; cluster algorithm: average linkage).

Transcription Factor, Network, and Canonical Pathway Analyses. Transcription factor prediction was carried out with the Upstream Regulator Analysis (URA) module of the Ingenuity Pathway Analysis (IPA) (set to the default setting). This analysis predicts, using the gene-expression data (i.e., group $\log_2$ ratios), the activation state of upstream transcription factors (i.e., 1,693 in Ingenuity Knowledge Base, Ingenuity Systems). A *z*-score is calculated, which determines whether the upstream transcription factor is statistically predicted to be "activated" or "inhibited" ($z > 0$ or $z < 0$, respectively). URA also provided bias analysis. Because the average bias was universally small (<0.25), bias-correction was not required and the activation *z*-score could be used for significance calling and to infer the (de)activation states.

We did this analysis for the male and female "stress exposure" and "exposure-related individual differences" probe sets separately, and then constructed an across-sex transcription factor signature for each tissue by pulling together male and female predicted transcription factors (Dataset S2 *A–C*). We then constructed the union and intersection of the three individual differences transcription-factor lists (Datasets S2*D* and S3*E*, respectively), identified the top targeted genes of the nine converging across-tissue transcription factors (Dataset S2*F*), and performed gene network analysis using GeneMania at the default setting (9). Network data are presented in Dataset S3 *A–C* and were visualized in Cytoscape (10) and presented in Fig. 2. Finally, the three transcription-factor lists (Dataset S4 *B–D*) were submitted to an IPA Canonical Pathway Analysis (default setting).

1. Cohen H, et al. (2006) Blunted HPA axis response to stress influences susceptibility to posttraumatic stress response in rats. *Biol Psychiatry* 59(12):1208–1218.
2. Cohen H, Matar MA, Buskila D, Kaplan Z, Zohar J (2008) Early post-stressor intervention with high-dose corticosterone attenuates posttraumatic stress response in an animal model of posttraumatic stress disorder. *Biol Psychiatry* 64(8):708–717.
3. Cohen H, Zohar J (2004) An animal model of posttraumatic stress disorder: The use of cut-off behavioral criteria. *Ann N Y Acad Sci* 1032:167–178.
4. Cohen H, Zohar J, Matar M (2003) The relevance of differential response to trauma in an animal model of posttraumatic stress disorder. *Biol Psychiatry* 53(6):463–473.
5. Cohen H, Zohar J, Matar MA, Kaplan Z, Geva AB (2005) Unsupervised fuzzy clustering analysis supports behavioral cutoff criteria in an animal model of posttraumatic stress disorder. *Biol Psychiatry* 58(8):640–650.
6. Cohen H, et al. (2004) Setting apart the affected: The use of behavioral criteria in animal models of post traumatic stress disorder. *Neuropsychopharmacology* 29(11): 1962–1970.
7. Paxinos G, Watson C (2007) *The Rat Brain in Stereotaxic Coordinates* (Elsevier Academic, San Diego), 6th Ed.
8. Du P, Kibbe WA, Lin SM (2008) lumi: A pipeline for processing Illumina microarray. *Bioinformatics* 24(13):1547–1548.
9. Warde-Farley D, et al. (2010) The GeneMANIA prediction server: Biological network integration for gene prioritization and predicting gene function. *Nucleic Acids Res* 38(Web Server issue):W214–220.
10. Montojo J, et al. (2010) GeneMANIA Cytoscape plugin: Fast gene function predictions on the desktop. *Bioinformatics* 26(22):2927–2928.

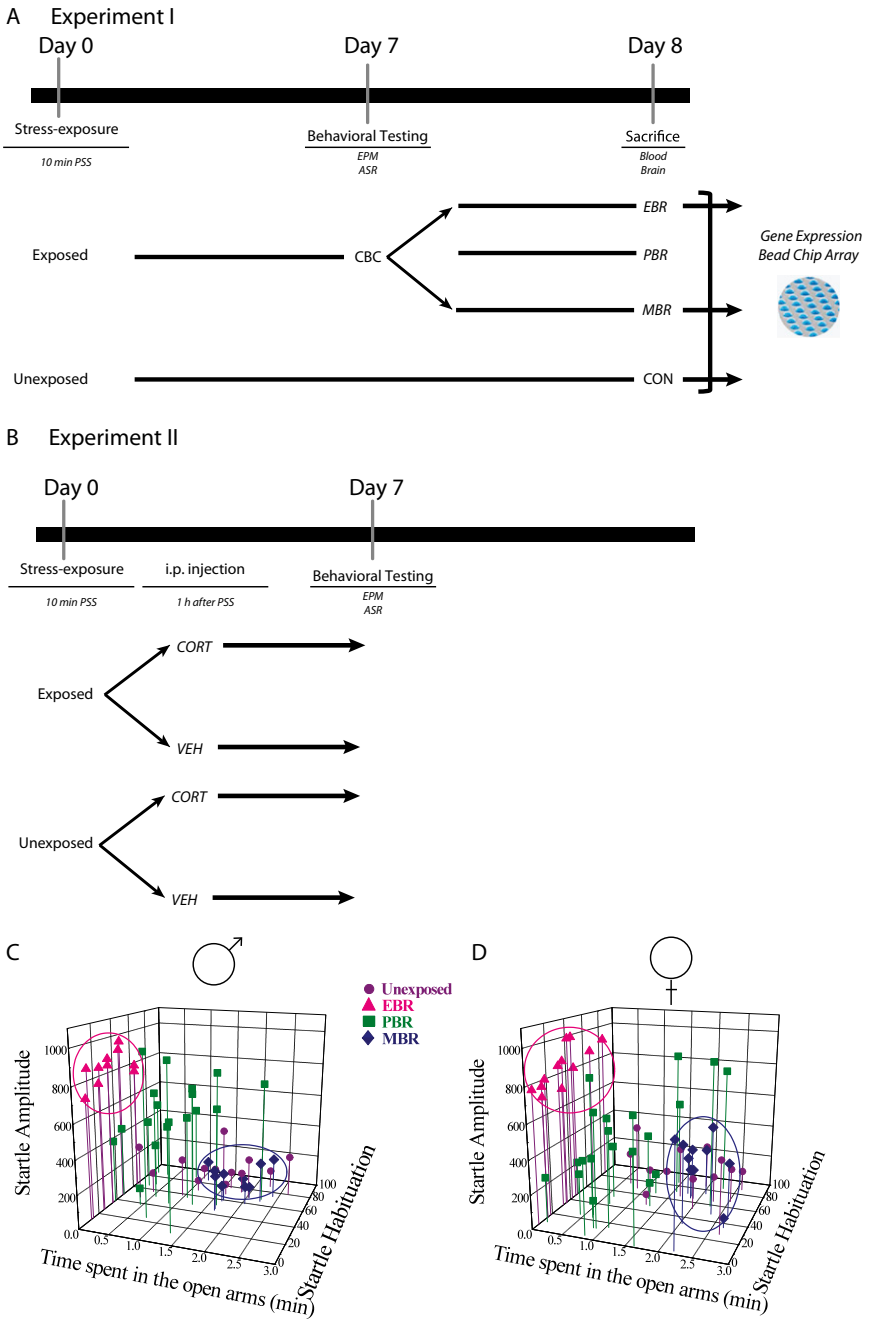

Fig. S1. (*A*) Experiment I design. Naïve adult male and female Sprague–Dawley rats were exposed to 10 min of PSS on day 0. Seven days after (day 7), they were behaviorally tested under basal conditions using the EPM and the ASR tests together with unexposed CONs. According to CBC, PSS-exposed rats were subdivided in rats displaying an EBR, PBR, and MBR to PSS. The day after (day 8), PSS-exposed rats and CONs were killed; RNA from dissected amygdalae and hippocampi and blood of EBRs, MBRs, and CONs were used for gene expression profiling using the Illumina Bead Chip Array. (*B*) Experiment II design. Naïve adult male and female Sprague–Dawley rats were exposed to PSS or remained unexposed to stress on day 0. One hour after, they were intraperitoneally injected with high dose (25 mg/kg) corticosterone (CORT) or vehicle (VEH) solution. Seven days after (day 7), they were behaviorally tested under basal conditions using the EPM and ASR tests. (*C* and *D*) Characterization of the behavioral response to PSS in male (*C*) and female (*D*) rats. Behavioral data of PSS-exposed and PSS-unexposed rats are depicted in three-dimensions: the *x* axis represents time spent in the open arms of the EPM, the *y* axis represents ASR-amplitude, and the *z* axis represents ASR-habituation. Triangles represent the EBRs, diamonds represent the MBRs, squares represent the PBRs, and circles represent the unexposed CONs.

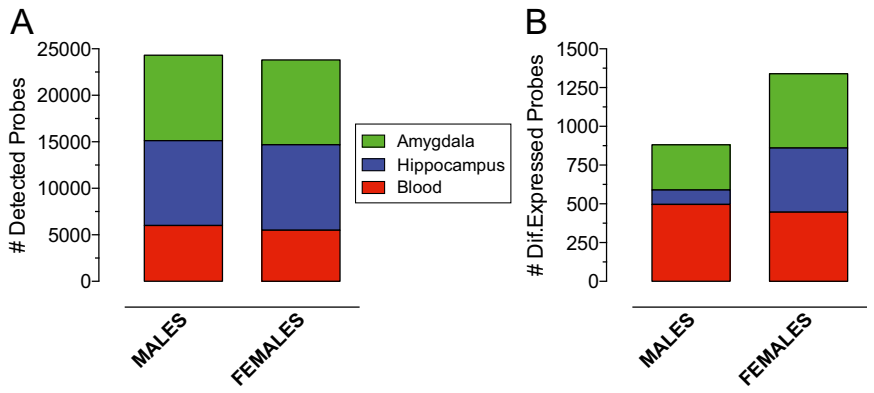

Fig. S2. Number (#) of detected (*A*) and differentially expressed (*B*) probes per tissue per sex.

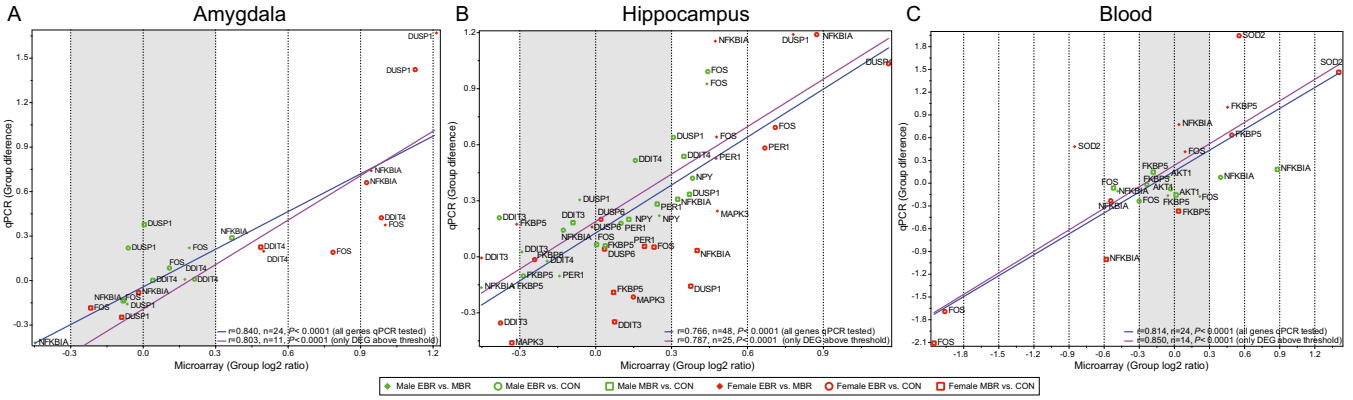

Fig. S3. Correlations between microarray $\log_2$ ratios of the group geometric means (*x* axis) and qPCR group differences in expression (*y* axis) in amygdala (*A*), hippocampus (*B*), and blood (*C*). The blue least-squares line takes into account data from all genes tested by qPCR, including DEG above the $\log_2$ ratio cut-off (i.e., absolute value greater than 0.3), DEG below the $\log_2$ ratio cutoff, and non-DEG. The purple least-squares takes into account only DEG above the $\log_2$ ratio cut-off. Two correlation coefficients (R) are indicated in each graph, as well as the respective *P* values and the number (*n*) of measurements. Datapoints are marked based on which gene and type of comparison is represented. Green data points represent male data, whereas red represent female data. Diamonds represent data derived from the comparison of the EBR and MBR groups, circles represent data from the comparison of the EBR and CON groups, and squares represent data from the comparison of the MBR and CON groups. The raw microarray and qPCR data used for the graphs can be found in Dataset S1*G*.

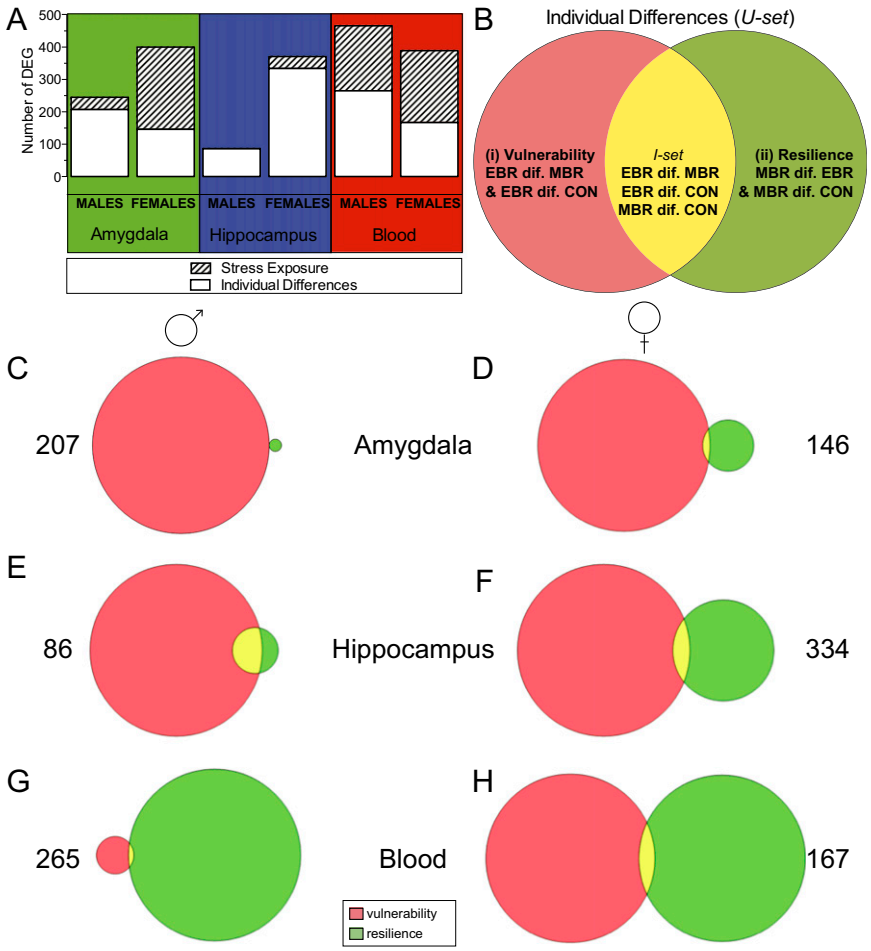

Fig. S4. Number of DEG associated with stress exposure (box with hatched lines) vs. exposure-related individual differences (empty box) per tissue per sex (*A*). The Venn-diagram template in *B* depicts the characteristics of DEG associated with: (*i*) vulnerability, where EBRs were different from both MBRs and CONs, and (*ii*) resilience, where MBRs were different from both EBRs and CONs. Their intersection contains DEG for which EBRs were different from MBRs and both EBRs and MBRs were different from CONs. Area-proportional Venn diagrams of the comparison of vulnerability- and resilience-related DEG in all tissue (amygdala, hippocampus and blood) and in both sexes are depicted in *C*–*H* (males: *C*, *E*, and *G*; females: *D*, *F*, and *H*). The number of genes in the union of the vulnerability-related DEG and the respective resilience-related DEG is indicated on the left of the left panels and on the right of the right panels.

A

Amygdala Transcription Factors predicted Signaling		
TOP-10 Canonical Pathways	*-log(P value)*	*# molecules*
Glucocorticoid Receptor Signaling	1.11E01	10
Aryl Hydrocarbon Receptor Signaling	1.03E01	8
Molecular Mechanisms of Cancer	9.97E00	10
Colorectal Cancer Metastasis Signaling	8.37E00	8
MIF Regulation of Innate Immunity	8.19E00	5
Role of Macrophages, Fibroblasts and Endothelial Cells in Rheumatoid Arthritis	7.59E00	8
Toll-like Receptor Signaling	7.49E00	5
PI3K Signaling in B Lymphocytes	7.23E00	6
CD40 Signaling	7.23E00	5
Estrogen-Dependent Breast Cancer Signaling	7.23E00	5

B

Hippocampus Transcription Factors predicted Signaling		
TOP-10 Canonical Pathways	*-log(P value)*	*# molecules*
Prostate Cancer Signaling	1.19E01	8
Glucocorticoid Receptor Signaling	9.29E00	9
ATM Signaling	9.04E00	6
Hypoxia Signaling in the Cardiovascular System	8.79E00	6
Aryl Hydrocarbon Receptor Signaling	8.37E00	7
ERK/MAPK Signaling	7.48E00	7
p38 MAPK Signaling	7.26E00	6
Estrogen-Dependent Breast Cancer Signaling	7.07E00	5
PI3K Signaling in B Lymphocytes	7.05E00	6
ERK5 Signaling	7.04E00	5

C

Blood Transcription Factors predicted Signaling		
TOP-10 Canonical Pathways	*-log(P value)*	*# molecules*
Glucocorticoid Receptor Signaling	1.57E01	15
Aryl Hydrocarbon Receptor Signaling	1.3E01	11
Prolactin Signaling	1.24E01	9
Role of Macrophages, Fibroblasts and Endothelial Cells in Rheumatoid Arthritis	1.19E01	13
PI3K Signaling in B Lymphocytes	1.18E01	10
Activation of IRF by Cytosolic Pattern Recognition Receptors	1.12E01	8
Estrogen-Dependent Breast Cancer Signaling	1.12E01	8
Role of PKR in Interferon Induction and Antiviral Response	1.09E01	7
B Cell Receptor Signaling	1.08E01	10
LPS-stimulated MAPK Signaling	1.07E01	8

Fig. S5. Top-10 predicted canonical pathways from amygdala (*A*), hippocampus (*B*), and blood (*C*) transcription factors associated with individual differences in the behavioral response to PSS. The enrichment Fischer's exact test *P* value is indicated, as well as the number of molecules (i.e., transcription factors) that contributed to the pathway enrichment.

Table S1. qPCR primers' target sequences and associated Universal Probe Library (UPL) probes

Gene symbol	Gene name	Gene type	Target mRNA sequence*	UPL Probe*
AKT1	V-akt murine thymoma viral oncogene homolog 1	Target	aacgacgtagccattgtgaaggagggctggctgcacaaa-cgaggggaatatattaaaacctggcggccacgctact-tcctcctcaagaatgatgg	71
DDIT3	DNA-damage-inducible transcript 3	Target	accaccacacctgaaagcagaaaccggtccaattacagt-catggcagctgagtctctgcctttcgcctttgagaca-gtgtccagct	13
DDIT4	DNA-damage-inducible transcript 4	Target	ccagagaagagggccttgaccgctgcgcgagcctggaga-gctcggactgcgagtccctggacagcagcaacagtgg-ctttgggccggaggaagactcctcatacctggatgg	80
DUSP1	Dual specificity phosphatase 1	Target	gtgcctgacagtgcagaatccggatgcagctcctgtagc-acccctctctacgaccaggggggcccagtggagatcc-tgtccttcctgtacctgg	17
DUSP6	Dual specificity phosphatase 6	Target	caggtggagagtcggtcctcgggctgctgctcaagaaac-tcaaagacgagggctgccgggcgttctaccttgaagg-tggcttcagtaagttccaggccg	66
FKBP5	FK506 binding protein 5	Target	ctcaaaccccaatgaaggagccacggtggaagtccacc-tggaaggctgctgtgctggaagggtgtttgactgc	66
FOS	FBJ murine osteosarcoma viral oncogene homolog	Target	gggacagcctttcctactaccattccccagccgactc-cttctccagcatgggctcccctgtcaacacacag-gacttttgcgcagatc	67
MAPK3	Mitogen-activated protein kinase 3	Target	ggaggtggaggtggtgaaggggcagccattcgacgtgg-gcccacgctacacgcagctgcagtacatcggcgagg-gcgcgtacggcatggtcagctcagcatatgaccacgtgc	46
NFKBIA	Nuclear factor of kappa light polypeptide gene enhancer in B-cells inhibitor, α	Target	gaaggagctgcgggagatccgcctgcagccgcaggag-gcgcctctggctgccgagccctggaagcaacagctc-acggaggacggagactcgttcctgcacttggcaatc	71
NPY	Neuropeptide Y	Target	ccgctctgcgacactacatcaatctcatcaccag-acagagatatggcaagagatccagccctgagaca	9
PER1	Period circadian clock 1	Target	gtgggcttgacacctcttctgtggcgccttcagcccct-ggttgccaccatggccccattccctctggtcgccgac-accactgccgatctaaagca	41
SOD2	Superoxide dismutase 2, mitochondrial	Target	tggacaaacctgagccctaagggtggtggagaacccaaa-ggagagttgctggaggctatcaagcgtgactttgggtc	67
B2M	Beta-2 microglobulin	Reference	agcaggttcctcaaacaagggtccagaggaaagggactaa-gaaaggactccaaggcagaa	6
HPRT1	Hypoxanthine phosphoribosyltransferase 1	Reference	gaccggttctgtcatgtcgaccctcagtcccagcgtcgt-gattagtgatgatgaaccaggt	95

*Gene expression primers and probes were designed based on the National Center for Biotechnology Information sequence (NM_004117.2) using the ProbeFinder v2.49 software (Roche, www.roche-applied-science.com).

Dataset S1. Differential gene expression results

Dataset S1

(*A*–*C*) Differentially expressed probes in males; (*D*–*F*) differentially expressed probes in females; (*G*) raw qPCR data and calculated values for Fig. S3.

Dataset S2. IPA upstream regulator analysis

Dataset S2

Transcription factors identified in amygdala (*A*), hippocampus (*B*), and blood (*C*). (*D*) Between-tissue overlap of transcription factors associated with exposure-related individual differences together with their canonical pathway annotation. (*E*) Across-tissue convergent transcription factors associated with exposure-related individual differences and their DEG targets. (*F*) Ranking of the DEG targets of the across-tissue convergent transcription factors.

Dataset S3. GeneMANIA network results for the identified amygdala (*A*), hippocampus (*B*), and blood (*C*) transcription factors associated with exposure-related individual differences

Dataset S3

Dataset S4. IPA canonical pathways

Dataset S4

(*A*) Common canonical pathways of the identified transcription factors associated with exposure-related individual differences. Enriched canonical pathways from amygdala (*B*), hippocampus (*C*), and blood (*D*) transcription factors associated with exposure-related individual differences.